Climate and Hydrology

Potential Climate Change Effects on Water Tables and Pyrite Oxidation in Headwater Catchments in Colorado

Richard M.T. Webb, M. Alisa Mast, Andrew H. Manning, David W. Clow, Donald H. Campbell

Abstract

A water, energy, and biogeochemical model (WEBMOD) was constructed to simulate hydrology and pyrite oxidation for the period October 1992 through September 1997. The hydrologic model simulates processes in Loch Vale, a 6.6-km² granitic watershed that drains the east side of the Continental Divide. Parameters describing pyrite oxidation were derived sulfate concentrations measured in pore water and stream water in Handcart Gulch, a naturally acidic watershed in the Colorado Mineral Belt. Average monthly differences in precipitation and temperature between current and future climates, as predicted by using six global circulation models and three carbon-dioxide emission scenarios, were input into WEBMOD to identify possible shifts in the quantity and quality of the water flowing from the watershed for the period 2005 through 2100. Initial results suggest that increased air temperatures will result in earlier snowmelt compared to current conditions. Average sulfate concentrations and acidity in streams draining hydrothermally altered terrain may decrease as water tables rise in response to greater overall precipitation and earlier snowmelt, although a net increase of sulfate load was simulated as a result of greater overall discharge. Evapotranspiration is expected to increase but not enough to offset the increase in precipitation.

Introduction

Concentrations of metals in the water and sediments in Handcart Gulch and other naturally acidic streams in the Colorado Mineral Belt are often found at levels that are toxic to fish and other aquatic organisms (Figure 1; Church et al. 2009, Schmidt et al. 2009). The present study uses numerical simulations to examine how climate change may affect the oxidation of pyrite and its acid-producing potential in these streams. Because hydrologic observations in Handcart Gulch are in the preliminary stages, the geochemistry determined for Handcart Gulch was inserted into a hydrologic model of Loch Vale that was built using temperature, precipitation, and discharge observations for the water years 1993 through 1997.

The Loch Vale watershed drains the eastern slope of the Colorado Front Range in Rocky Mountain National Park near Estes Park, CO. Within the 6.6-km² watershed (Figure 1), elevations rise from 3,000 meters (m) above mean sea level (amsl) at the watershed outlet (the Loch) to 4,000 m amsl along the Continental Divide. The watershed contains a small cirque glacier and a rock glacier that occupy the topographically shaded northeastern facing slopes. In western North America, snowpack has declined in recent decades, and this trend is expected to continue through the 21st century (Pederson et al. 2011). Mean annual air temperatures at Loch Vale have risen 1.2–1.4°C since 1990, resulting in earlier spring melts and the release of water previously locked up in permafrost above 3,460 m amsl (Clow et al. 2003).

Handcart Gulch is a naturally acidic stream that drains hydrothermally altered terrain on the eastern flank of the Continental Divide 90 km south of Loch Vale (Caine et al. 2008). Elevations in the watershed vary from 3,200 m at the gage to 3,700 m amsl. Similar to Loch Vale, a rock glacier flows down the valley. Using cations, including H_3O^+, is an order of magnitude greater at Handcart Gulch than at Loch Vale. Of course, alpine watersheds are not steady state; instead they display large variations of flow and concentration as snowpack builds through the winter and melts in the summer. Numeric watershed models that simulate

Webb, Mast, Manning, Clow, and Campbell are research scientists with the U.S. Geological Survey, Box 25046, Denver Federal Center, Denver, CO 80225. Webb, MS412; Mast, MS 415; Manning, MS 973; Clow, MS 415; Campbell, MS 418. Emails: rmwebb@usgs.gov; mamast@usgs.gov; amanning@usgs.gov; dwclow@usgs.gov; dhcampbe@usgs.gov.

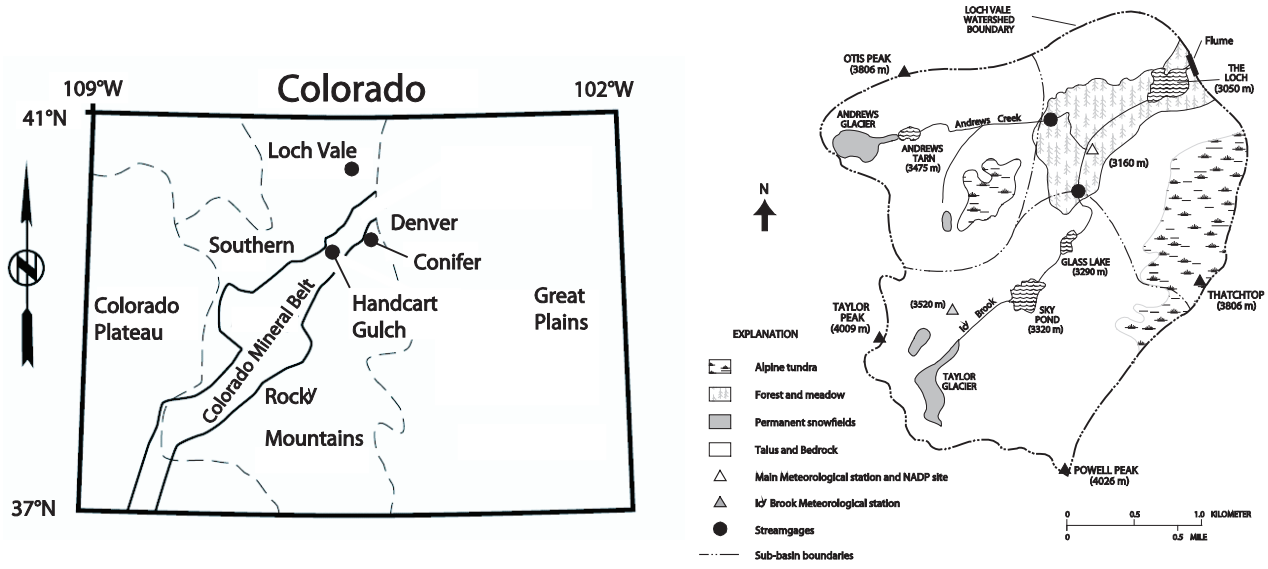

Figure 1. Location of Loch Vale and Handcart Gulch in relation to major geomorphic and mineralogic provinces in Colorado (modified from Church et al. 2009) and descriptive map of the Loch Vale watershed (modified from Campbell et al. 1995).

steady-state estimates described below, the export of hydrologic and geochemical fluxes and states on a daily time step provide an important tool to better understand the cause and effect of these variations.

Methods

Possible changes in the hydrology and pyrite oxidation of mineralized watersheds were simulated by shifting the temperature and precipitation observed for water years 1993 through 1997 to the temperature and precipitation predicted by six general circulation models (GCMs), each running three different carbon dioxide emission scenarios for the 21st century. The construction of a Handcart Gulch hydrologic model is in the preliminary stages, reflecting the limited observations of flow and water quality at the basin outlet. So for this study, Loch Vale was used as a hydrologic proxy for Handcart Gulch, which has similar elevations and air temperatures. Pyrite concentrations and weathering rates estimated for Handcart Gulch were added to the Loch Vale model to simulate annual variations in water quality in alpine and subalpine watersheds underlain by mineralized deposits.

WEBMOD

The Water Energy and Biogeochemical Model (WEBMOD) is a semidistributed watershed model that simulates hydrology and geochemistry on a daily timestep (Figure 2; Webb et al. 2006).

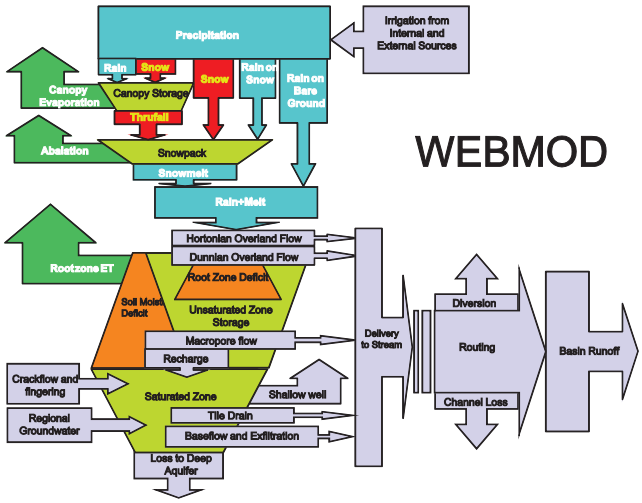

Figure 2. Reservoirs and fluxes of WEBMOD. Infiltration, transpiration, and wetting of the root zone by groundwater are not shown to simplify the schematic.

Insolation, temperature, precipitation, potential evapotranspiration, and canopy interception and evaporation are distributed to hillslopes by using algorithms from the U.S. Geological Survey's Precipitation Runoff Modeling System (PRMS; Leavesley et al. 1983, Leavesley and Stannard 1995). Snowpack accumulation and melt are simulated with the National Weather Service's Hydro-17 snow module (Anderson 1973). Hillslope processes including overland flow, infiltration, evaporation and transpiration, shallow return flow, and base flow are

simulated with the variable source area model TOPMODEL (Beven and Kirkby 1979, Wolock 1993, Beven 1997). Hillslope discharge is routed to the basin outlet by using a unit hydrograph (Clark 1945). Mixing ratios from the hydrologic model are used to simulate the transient aqueous geochemistry in each hydrologic compartment using PHREEQC (Parkhurst et al. 1999, Charlton and Parkhurst 2011).

Hydrologic Model

The Loch Vale watershed was discretized into six hillslopes representing southern (warmer) and northern (cooler) exposures for Andrews Creek, Icy Brook, and the Loch area downstream from the confluence. Five years of meteorological observations from a weather station in the watershed were used to drive the simulations of evapotranspiration, snowpack processes, hillslope processes, and runoff from October 1992 through September 1997. Annual precipitation during the period averaged 128 cm with 60 percent falling mostly as snow from late autumn through spring (November through May). WEBMOD process parameters were adjusted to reproduce the dominant hydrologic processes in the basin including the accumulation of snowpack in the winter, the initial rise of soil moisture in the spring, and melting of the snowpack in the spring and summer (Figure 3). The sharp rise in observed runoff beginning in the middle of May marks the breakup of ice in the flume at the outlet of the Loch. There are no ice dam dynamics in WEBMOD, so simulated runoff increases earlier than observed runoff. Runoff decreases as the snowpack becomes depleted, first near the Loch and progressing up Icy Brook and Andrews Creek. The temperature lapse rate between two weather stations in the watershed, the Main weather station (3,160 m amsl) and the Icy Brook weather station (3,520 m amsl), for water year 1994 was approximately 10°C/km in the winter and 6°C/km during the summer.

Simulated snowpack begins accumulating in September and reaches a maximum of approximately 60 cm of snow-water equivalence at the end of April (Figure 4). A basin average snow-water equivalence of 60 cm is equal to 1.7 m of snow depth using an average density of 35 percent. Because of the extreme relief and high winds, the depth of snowpack varies greatly, with basin-wide snow-covered area rarely exceeding 75 percent.

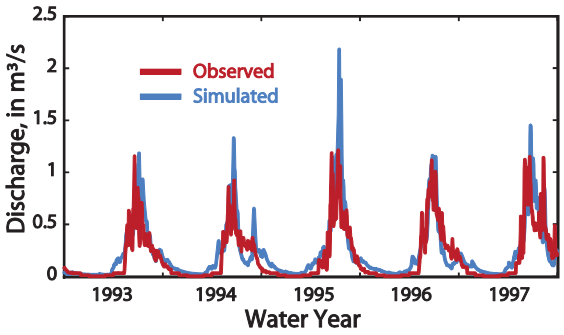

Figure 3. Observed versus simulated discharge for Loch Vale for the water years 1993–1997. The abrupt beginning of runoff observed in the spring corresponds to the melting of the ice dam in the flume.

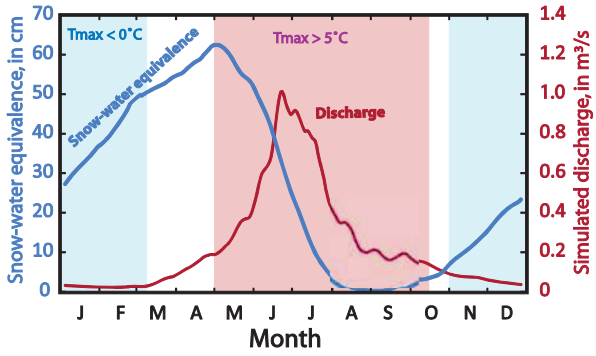

Figure 4. Average daily simulated snow-water equivalence and discharge at Loch Vale for the water years 1993–1997. Values are moving averages centered on 9-day periods. Shading indicates daily maximum temperatures at the Main weather station (blue, <0°C; white, 0°C<tmax<5°C; red, >5°C).

The onset of partial thawing of the watershed begins in March, as documented by rising soil moisture saturation that corresponds to rising spring temperatures and rain on snow events (Figure 5). Soil moisture reaches a maximum during spring melt and then drops in response to evapotranspiration (ET) demand through the summer. Soil moisture begins to rise in late summer, possibly in response to monsoonal moisture and (or) decreased transpiration rates due to the closing of stoma by stressed conifers. Sap-flow sensors installed in lodgepole pines at an elevation of 2,500 m near Conifer, CO, indicated a transpiration season of April 8–October 12 in 2000 and April 18–September 28 in 2001 (Bossong et al. 2003).

In the WEBMOD simulations for the higher and cooler elevations of Loch Vale, transpiration was set to begin at the beginning of June and end at the beginning of August. Because the area covered by tundra, grass, and conifers is limited for Loch Vale, transpiration is a

relatively minor fraction of overall ET in the model simulations. The reader should note the water-table fluctuations of less than a meter, shown in Figure 5, are computed for porosities typical of sandy clay loams or silty loams found in valley bottoms (porosity 0.4 with a field capacity of 0.2). Porosities in the WEBMOD implementation of TOPMODEL are constant for a hillslope, but the water-table fluctuations in the fractured rocks near the Continental Divide could be several tens of meters given measured porosities less than 0.05.

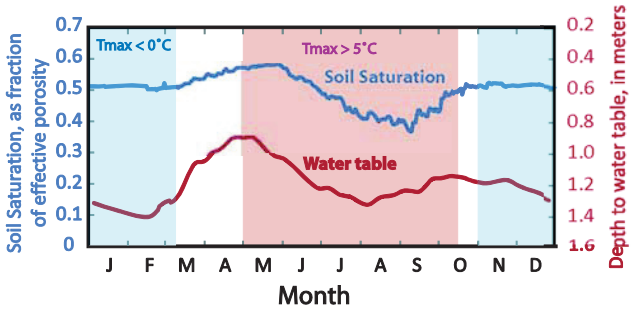

Figure 5. Average daily observed soil saturation for water years 1998–2002 and simulated depth to water table for water years 1993–1997. Values are moving averages centered on 9-day periods. Shading indicates daily maximum temperatures at the Main weather station (blue, <0°C; white, 0°C<tmax<5°C; red, >5°C).

Pyrite Weathering

Sulfate concentrations in precipitation falling on the Rocky Mountains are usually less than 20 µeq/L (approx. 1 mg/L) (National Atmospheric Deposition Program 2007). After interacting with the biotite gneiss and the Silver Plume granite (Cole 1977), slightly higher concentrations are measured in the waters exiting the Loch, implying that there is a certain amount of pyrite in the watershed (Mast 1992). In contrast, if the precipitation falls on hydrothermally altered terrain, sulfate in the springs and streams draining that terrain often exceed 1,000 µeq/L (approx. 50 mg/L). Figure 6 shows the dissolution of pyrite when exposed to oxygen as occurs in a mine tailings pile (Diehl et al. 2008). The dominant hydrothermal alteration assemblage at Handcart Gulch is quartz-sericite-pyrite (QSP) with an average concentration of about 8 weight-percent fine-grained, disseminated pyrite, FeS_2, and quartz-pyrite veinlets (Manning et al. 2009).

The three most sensitive factors in simulating pyrite weathering and the production of acidic waters in mineralized deposits are the mineral area to volume (A/V) ratio, the partial pressure of oxygen in the unsaturated zone, and the total mass of pyrite available for oxidation. Heterogeneities in abundance of pyrite and fracture apertures at both large and small scales make the knowledge of these data at all points in the watershed impossible. The values assigned to these parameters in the model, such as 5.0 dm^2/dm^3 for the A/V ratio, therefore, represent 'effective' values that are calibrated such that simulated values for pH and sulfate concentrations match those observed in the monitoring wells and and stream samples from Handcart Gulch (Manning et al. 2010). In these model runs, the initial mass of available pyrite is assigned an arbitrary value of 1.0 mol/kg, sufficient to ensure that the available pyrite will not be a limiting factor in the production of acidic waters during the simulation period of 5 years. Whereas pyrite abundance is not a limiting factor, the availability of oxygen is. In a thick unsaturated zone where pyrite is present, weathering consumes oxygen faster than diffusion can replace it, resulting in decreased oxygen and reduced weathering rates with depth (Figure 7).

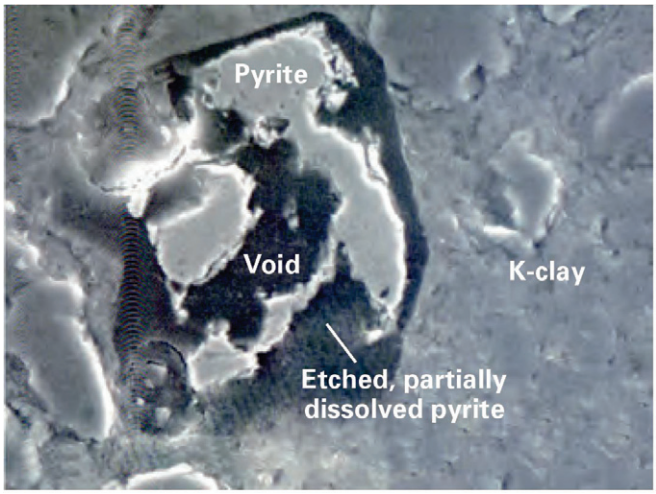

Figure 6. Partial dissolution of pyrite grain from the Dinero Mine waste pile (Diehl et al. 2008)

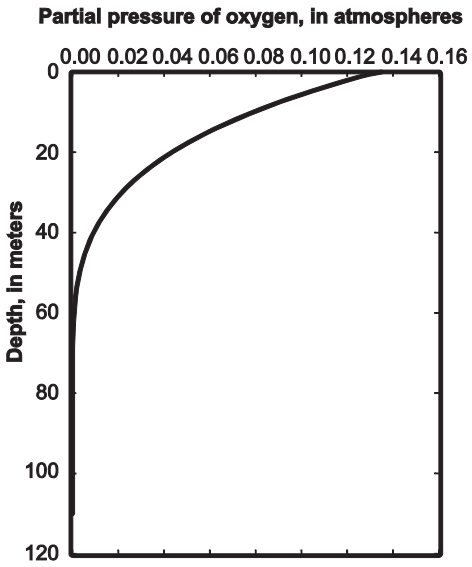

Figure 7. Plot showing decreasing oxygen with depth typical of values measured in deep unsaturated zones in the Handcart Gulch watershed.

To represent this process, pore waters in the unsaturated zone were equilibrated with oxygen partial pressures from 0.08 to 0.003 atmospheres depending on the their thickness.

The simplest form of pyrite oxidation was assumed:

$$FeS_{2(s)} + 3.5\ O_2 + H_2O \rightarrow Fe^{2+} + 2\ SO_4^{2-} + 2\ H^+$$

As a result of the oxidation of pyrite, the pH of the perennial stream draining the Handcart Gulch varies between 3 and 4. Using an average pH of 3 ($[H^+]$ = 1 meq/L), a sulfate concentration of 50 mg/L ($[SO_4^{2-}]$~1 meq/L), and a mean discharge of 46 L/s (unpublished data for water year 2005) at the outlet of a watershed area of 3.6 km², the annual export of hydrogen from Handcart Gulch exceeds 4,000 eq/ha/yr with similar yields of sulfate.

Williamson and Rimstidt (1994) added extensive laboratory observations to the existing body of literature to arrive at the following empirical empirical kinetic rate expression for the above reaction (appropriate for the pH range 2–10):

$$r'_{25°C} = 10^{-8.19(\pm 0.10)} * \frac{m_{DO}^{0.5(\pm 0.04)}}{m_{H^+}^{0.11(\pm 0.01)}},$$

where $r'_{25°C}$ is the rate of pyrite weathering in mol/m²/s, and concentrations, *m*, of dissolved oxygen and hydrogen (as a hydronium ion H_3O^+) are in mol/kg of water at 25°C. The rate exponent of -8.19 describes the rate at 25°C for 1 m² of pyrite surface area per kg of solution. The pyrite kinetic weathering rate used in the WEBMOD simulations was

$$r'_{2°C} = 10^{-9.14} * \frac{5.0 m_{DO}^{0.5}}{m_{H^+}^{0.11}}.$$

The exponent of -9.14 was computed by using the Arrhenius equation (Arrhenius 1889) with an activation energy for pyrite of 65 kJ/mol to convert the rate constant at 25°C to 2°C, an average soil temperature at Handcart Gulch. The coefficient of 5.0 is the effective surface area to volume (A/V) ratio, in PHREEQC units of dm²/dm³, estimated for the QSP deposits at Handcart; A/V equals 100.0 dm²/dm³ (≅ 1 m²/kg) in the Williamson and Rimstidt paper.

Using transition-state theory (Eyring 1935), the computed kinetic reaction rate is further reduced as pyrite approaches saturation:

$$r = r'_{2°C} * (1 - SR^n),$$

where *r* is the rate of pyrite weathering in mol/m²/s, $r'_{2°C}$ is the empirical rate constant in mol/m²/s at 2°C, SR is the saturation ratio that ranges from 0.0 for no dissolved ions to 1.0 when the solution is in equilibrium with pyrite, and *n* is a coefficient to account for other factors, set to 1 in this case.

Coupled Hydrology and Geochemistry

The unsaturated and saturated zones were initialized with major-ion concentrations similar to those measured in samples from monitoring wells in the Handcart Gulch watershed. Both zones were assigned identical pyrite abundance (1 mol/kg), A/V ratios (5.0 dm²/dm³), and kinetic expressions. Unsaturated zones were in equilibrium with depleted atmospheric oxygen as described above. Oxygen in the saturated zone, however, was limited to that contained in recharge water draining from the unsaturated zone; diffusion of oxygen into the saturated zone was considered negligible. After initializing the water quality and geochemistry, the daily simulations begin with the atmospheric deposition using concentrations measured at Loch Vale, one of the closest sites where precipitation chemistry is routinely measured (National Atmospheric Deposition Program 2007). Simulated fluxes between compartments shown in Figure 2 were used to provide mixing ratios for a series of forward-feeding batch reactions: Precipitation > Canopy > Snowpack > Overland Flow > Unsaturated Zone > Saturated Zone > Stream. On days with no precipitation, transpiration would move water and solutes to the canopy. For all compartments the batch reactions proceed as follows: inputs are conservatively

mixed with existing storage, the mixed solution is exported to downstream compartments, and reactions then take place in the final volume. During the reaction calculations, ions released by the oxidation of pyrite can precipitate out as goethite, kaolinite, montmorillinite, and (or) calcite when thermodynamically stable.

Net exports of sulfate will closely match the shape of the hydrograph (Figure 4) as the loads are dependent on discharge, which varies over orders of magnitude, and concentration, which is predicted to vary less. Simulated sulfate concentrations in the unsaturated zone varied between 20 and 60 mg/L with the greatest concentrations in late winter and late summer, coincident with lower water tables (Figure 8, Figure 5). Groundwater concentrations varied less, between 41 and 44 mg/L, and are predicted to lag the peak concentrations in the unsaturated zone by more than a month. The acidity of the streamwater in WEBMOD is a mixture of overland flow, the unsaturated zone, and groundwater (Figure 2); the simulated stream acidity varies throughout the year, reflecting relative contributions from each source (Figure 9).

Climate Models and Energy Scenarios

Greenhouse gas emissions continue to increase as fossil fuels are consumed by a global population that has grown from less than 2 billion in 1900 to almost 7 billion today. Warming of the climate system is unequivocal, as is now evident from observations of increases in global average air and ocean temperatures, widespread melting of snow and ice, and rising global average sea level (Intergovernmental Panel on Climate Change 2007). The main uncertainty is the degree of warming and the direction and magnitude of changes in precipitation. To address these uncertainties, six global climate models were run with three carbon dioxide emission scenarios using the climatologic downscaling and data synthesis of Hay et al. (2011) and Markstrom et al. (in press). Global climate models consist of coupled atmospheric and oceanic general circulation models sometimes linked with additional models that simulate aerosols, sea ice, glacial melting, land cover, and vegetation models. The acronym GCM that was originally used for general circulation models is now commonly used, as it is here, to describe the coupled global climate models. All models in this study (Table 1) are sensitive to the loads of greenhouse gases emitted by natural and anthropogenic sources.

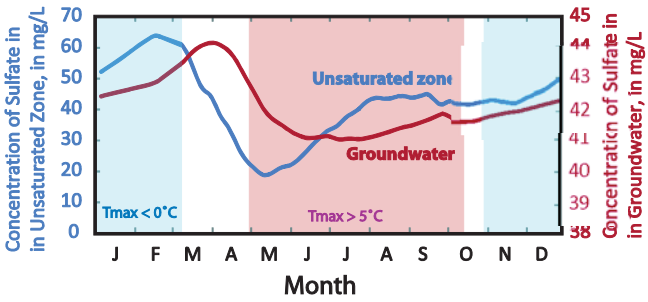

Figure 8. Average daily simulated concentration of sulfate in the unsaturated zone and groundwater for the the water years 1993–1997 for the Loch Vale hydrologic model with a hypothetical pyrite-bearing deposit. Values are moving averages centered on 9-day periods. Note that variations in unsaturated zone concentrations are ten times those simulated for groundwater. Shading indicates daily maximum temperatures at the Main weather station (blue, <0°C; white, 0°C<tmax<5°C; red, >5°C).

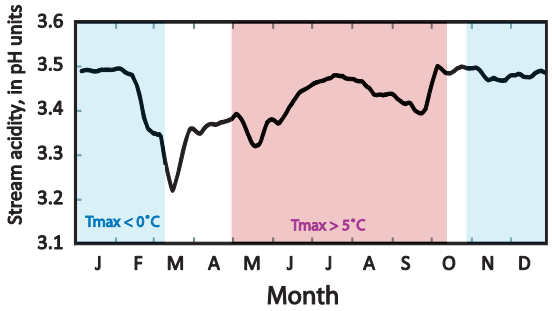

Figure 9. Average daily simulated stream acidity for the water years 1993–1997 for the Loch Vale hydrologic model with a hypothetical pyrite-bearing deposit. Values are moving averages centered on 9-day periods. Shading indicates daily maximum temperatures at the Main weather station (blue, <0°C; white, 0°C<tmax<5°C; red, >5°C).

Each GCM was validated by simulating the climate for the 20th century. In all cases, matching temperatures observed in the second half of the century required the input of anthropogenic greenhouse gases. The 20th century simulation, referred to as 20C3M for each GCM, forms the baseline to compute temperature and precipitation changes for each emission scenario of the 21st century. The WEBMOD simulation for water years 1993–1997 forms the hydrologic and geochemical baseline to quantify potential shifts in hydrology and oxidation of pyrite during warming climate conditions through the 21st century.

Table 1. GCM outputs used in this study from the World Climate Research CMIP3 multimodel dataset archive. (BCCR-BCM2.0, Bjerknes Centre for Climate Research Bergen Climate Model; CSIRO Mk3.0, Commonwealth Scientific and Industrial Research Organisation Mark version 3.0; INM-CM3.0, Institute of Numerical Mathematics Coupled Model, version 3.0; MIROC3.2(medres), Model for Interdisciplinary Research on Climate 3.2, medium-resolution version)

GCM*	Developer
BCC-BCM2.0	Bjerknes Centre for Climate Research, Norway
CCSM3	National Center for Atmospheric Research, USA
CSIRO-Mk3.0	Commonwealth Scientific and Industrial Research Organisation, Australia
CSIRO-Mk3.5	Commonwealth Scientific and Industrial Research Organisation, Australia
INM-CM3.0	Institute for Numerical Mathematics, Russia
MIROC3.2(medres)	National Institute for Environmental Studies, Japan

* CMIP3 GCM documentation, references, and links can be found online at http://www-pcmdi.llnl.gov/ipcc/model_documentation/ipcc_model_documentation.php.

Table 2. Three emission scenarios simulated by each of the six GCMs to simulate climate conditions for the 21st century (from Intergovernmental Panel on Climate Change 2007).

Scenario*	Description
20C3M	20th century climate used to determine baseline (1992–1997) conditions
A2	Very heterogeneous world with high population growth, slow economic development, and slow technological change
A1B	Very rapid economic growth, a global population that peaks in mid 21st century and rapid introduction of new and more efficient technologies with a balanced emphasis on all energy sources
B1	Convergent world, with the same global population as Emission Scenario A1B but with more rapid changes in economic structures toward a service and information economy that is more ecologically friendly

The three greenhouse gas emission scenarios used in this study (Table 2) range from pessimistic to optimistic in terms of slowing the rate of increase of annual emissions though a combination of slowing population growth, conservation practices, and new technology.

For each GCM and emission scenario, the average monthly difference in precipitation and temperature were computed between the baseline (20C3M for 1992–1997) and the 95 21st-century 5-year periods (2001–2005, 2002–2006, ..., 2095–2099). Those monthly differences were applied to the WEBMOD data to create 95 'future' 5-year simulations of hydrology and pyrite weathering for the six GCMs and three emission scenarios (1,710 model runs). Differences in monthly means of simulated hydrology and pyrite weathering were computed for the last 4 years of each model run; simulations of the first year were excluded to diminish artifacts resulting from initial conditions. To illustrate seasonal differences in watershed processes, baseline model runs for each GCM/scenario were compared to the monthly statistics for model runs centered on the years 2030, 2060, and 2090. Possible interannual variations and long-term trends were documented by plotting the means and range for each variable.

Results

All GCM/emission scenarios predict that average air temperature in Colorado will rise throughout the century; the mean increase for scenario B1 is approximately 2°C, whereas scenario A2 predicts 4°C (Figure 10).

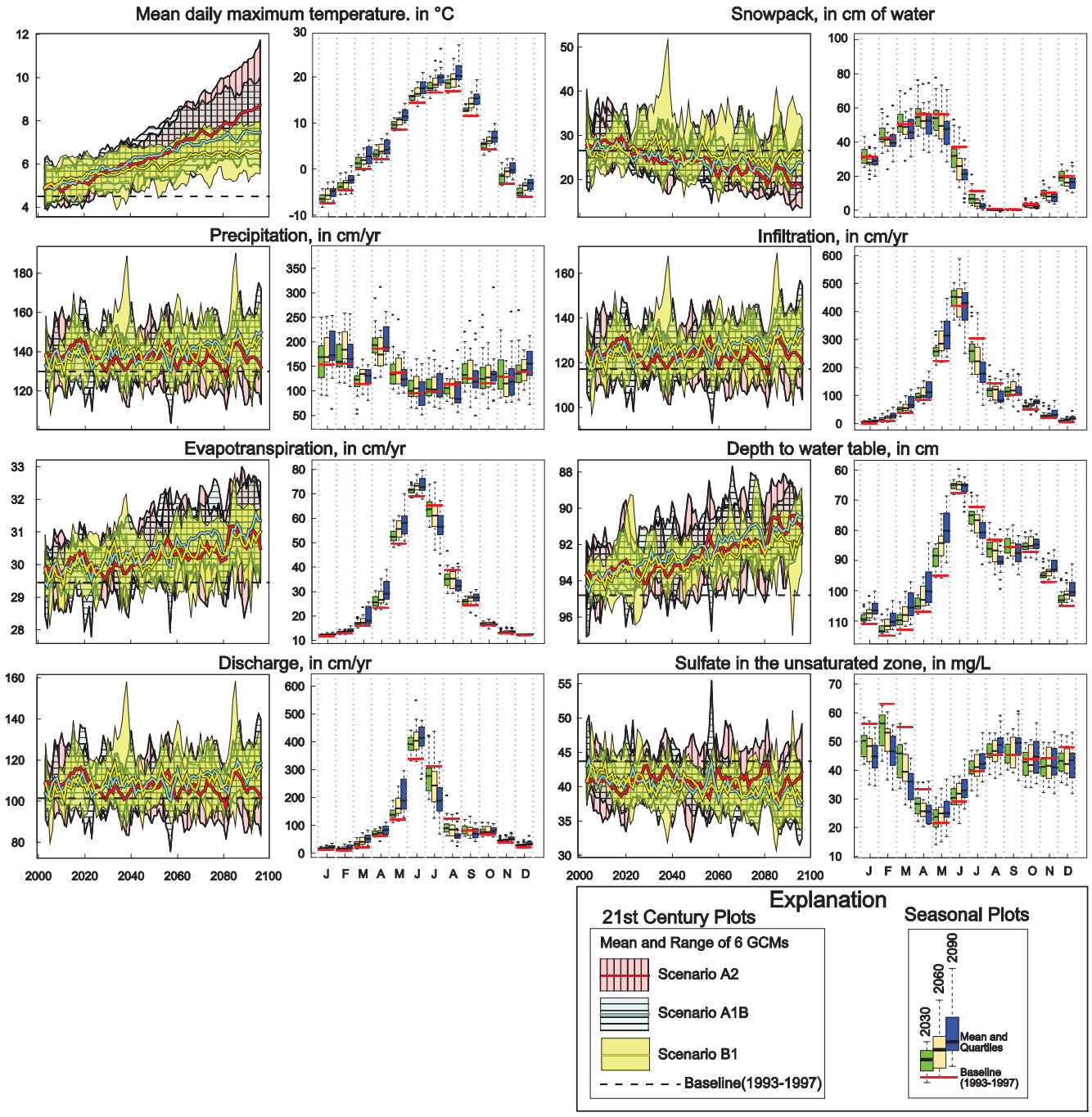

Figure 10. Interannual and seasonal differences between simulations of hydrology and sulfate production for climate observed for water years 1993–1997 and climate predicted by six global climate models using three different emission scenario.

The Clausius-Clapeyron equation (Clapeyron, 1834) dictates that a 2°C increase in average air temperature would result in approximately a 14 percent increase in water-holding capacity in the atmosphere (approx. 7%/K). The absolute increases in moisture amount should be greater at lower latitudes, but the additional moisture may not be available to extratropical storms creating precipitation over the Rocky Mountains (Trenberth et al. 2003). The GCMs simulating the A1B and the B1 scenarios predict an increase in mean annual precipitation of about 20 cm over the century (an increase of 15 percent over the mean baseline precipitation of 130 cm). The interannual trend of increasing precipitation is rather noisy, reflecting the complex interplay between albedo and the evaporation, advection, and precipitation of moisture around the globe. A plot of seasonal precipitation for all GCMs and scenarios for the years 2030, 2060, and 2090 shows most of the increase in precipitation occurring in the winter months. With the increased temperatures, a greater percentage of spring and fall precipitation may fall as rain, resulting in shallower snowpacks that will begin melting earlier in the spring. The shift in form (rain/snow) and timing of precipitation has significant implications for watersheds that respond to the buildup and melt of the seasonal snowpack.

Increasing temperature and precipitation would result in steadily increasing ET. Evapotranspiration is expected to exceed baseline conditions for all months except for July and August, when ET would be severely limited by available soil moisture. In response to the shift in the volume and timing of snowpack, the discharge from the watershed is expected to begin earlier and reach its peak earlier in the summer as available snowpack is depleted.

Given winters with more precipitation and warmer temperatures than present, infiltration is expected to increase for all months except for July and August when snowpack is depleted, precipitation is lower, and any available precipitation would be used to meet the high ET demand.

The increase in overall precipitation and infiltration that exceeds the increase in ET would result in a rising water table, again for all months except for July and August. A rising water table would reduce the volume of pyrite oxidation zone (for water table depths <50 m) and thus reduce overall concentrations of sulfate in the unsaturated and saturated zones. Concentrations would decrease for all months except for a slight increase from May through August as the water table lowers in response to depleted snowmelt. Overall, the loads of sulfate exported from the watershed would be greater than baseline.

Conclusions

A WEBMOD model was used to assess the effects of climate change on high-elevation mineralized Rocky Mountain watersheds. Baseline conditions describe a watershed with 60 percent of precipitation falling as snow with melting and runoff from May through September. In simulations using predicted climate changes, the percentage of precipitation falling as rain increased as did overall infiltration that recharges groundwater. Greater recharge resulted in reduced sulfate concentrations in the unsaturated and saturated zones for much of the year, although a net increase of sulfate load was simulated as a result of greater overall discharge. Evapotranspiration is expected to increase but not enough to offset the increase in precipitation. The simulations presented here assume no changes to the vegetation; if the vegetation shifts to one capable of transpiring significantly greater amounts of water given the same temperature and water availability, then the predicted rise in water table becomes less certain. The inclusion of more realistic plant and transpiration models into WEBMOD are high priorities.

Acknowledgments

The authors appreciate the assistance of the U.S. Geological Survey Modeling of Watershed System Project, who provided code and guidance on modifications needed to complete the climate change scenarios using WEBMOD.

References

Anderson, E.A. 1973. National Weather Service river forecast system: Snow accumulation and ablation model. National Oceanic and Atmospheric Administration Technical Memorandum NWS-HYDRO-17.

Arrhenius, S. 1889. .On the Reaction Velocity of the Inversion of Cane Sugar by Acids. Zeitschrift für Physikalische Chemie, v.4, 226-. as translated and published in Margaret H. Back & Keith J. Laidler, eds., Selected Readings in Chemical Kinetics. Oxford: Pergamon, 1967.

Beven, K.J. 1997. TOPMODEL: A critique. Hydrologic Processes 11(9):1069–1086.

Beven, K.J., and M.J. Kirkby. 1979. A physically based variable contributing area model of basin hydrology. Hydrology Science Bulletin 24(1):43–69.

Bossong, C.R., J.S. Caine, D.I. Stannard, J.L. Flynn, M.R. Stevens, and J.S. Heiny-Dash. 2003. Hydrologic conditions and assessment of water resources in the Turkey Creek watershed, Jefferson County, Colorado, 1998–2001. U.S. Geological Survey Water-Resources Investigations Report 03–4034.

Caine, J.S., A.H. Manning, P.L. Verplanck, D.J. Bove, K.G. Kahn, and S. Ge. 2008. U.S. Geological Survey research in Handcart Gulch, Colorado: An alpine watershed affected by metalliferous hydrothermal alteration. In P.L. Verplanck, ed. Understanding contaminants associated with mineral deposits, pp. 50–57. U.S. Geological Survey Circular 1328.

Campbell, D.H., D.W. Clow, G.P. Ingersoll, M.A. Mast, N.E. Spaher, and J.T. Turk. 1995. Processes controlling the chemistry of two snowmelt-dominated streams in the Rocky Mountains. Water Resources Research 31(11):2811–2821.

Charlton, S.R., and D.L. Parkhurst. 2011. Modules based on the geochemical model PHREEQC for use in scripting and programming languages. Computers and Geosciences, doi:10.1016/j.cageo.2011.02.005.

Church, S.E., D.L. Fey, T.L. Klein, T.S. Schmidt, R.B. Wanty, E.H. DeWitt, B.W. Rockwell, and C.A. SanJuan. 2009. Environmental effects of hydrothermal alteration and historical mining on water and sediment quality in central Colorado. In R.M.T. Webb and D.J. Semmens, eds. Planning for an uncertain future: Monitoring, integration, and adaptation. Proceedings of the Third Interagency Conference on Research in the Watersheds, pp. 85–95. U.S. Geological Survey Scientific Investigations Report 2009-5049.

Clark, C.O. 1945. Storage and the unit hydrograph: American Society of Civil Engineers Transactions 110:1419–1488.

Clapeyron, E. 1834. Puissance motrice de la chaleur, Journal de l'École Royale Polytechnique, Vingt-troisième cahier, Tome XIV, 153–190

Clow, D.W., L. Schrott, R.M.T. Webb, D.H. Campbell, A. Torizzo, and M. Dornblaser. 2003. Groundwater occurrence and contributions to streamflow in an alpine catchment. Ground Water 41(7):937–950.

Cole, J.C. 1977. Geology of the east-central Rocky Mountain National Park and vicinity, with emphasis on the emplacement of the Precambrian Silver Plume Granite in the Longs Peak–St. Vrain Batholith. Ph.D. dissertation, University of Colorado, Boulder, CO.

Diehl, S.F., P.L. Hageman, and K.S. Smith. 2008. What is weathering in mine waste?: Mineralogic evidence for sources of metals in leachates. In P.L. Verplanck, ed. Understanding contaminants associated with mineral deposits, pp. 4–7. U.S. Geological Survey Circular 1328.

Eyring, H. 1935. The Activated Complex in Chemical Reactions. Journal of Chemical Physics. 3:107.

Hay, L.E., S. L. Markstrom, and C.D. Ward-Garrison. 2011. Watershed-scale response to climate change through the 21st century for selected basins across the United States. Earth Interactions 15-017. [Available online at http://EarthInteractions.org.]

Intergovernmental Panel on Climate Change. 2007. Summary for policymakers. In S. Solomon, D. Qin, M. Manning, Z. Chen, M. Marquis, K.B. Averyt, M. Tignor, and H.L. Miller, eds. The physical science basis: Contribution of Working Group I to the Fourth Assessment Report of the Intergovernmental Panel on Climate Change, 18 pp. Cambridge University Press, Cambridge, UK, and New York, NY.

Leavesley, G.H., R.W. Lichty, B.M. Troutman, and L.G. Saindon. 1983. Precipitation-runoff modeling system: User's manual. U.S. Geological Survey Water-Resources Investigations Report 83-4238.

Leavesley, G.H., and L.G. Stannard. 1995. The Precipitation-Runoff Modeling System: PRMS. In V.P. Singh, ed. Computer Models of Watershed Hydrology, pp. 281–310. Water Resources Publications, Highlands Ranch, CO.

Madole, R.F. 1976. Glacial Geology of the Front Range, Colorado. In W.C. Mahaney, ed. Quaternary Stratigraphy of North America, pp. 297–318. Dowden, Hutchinson, & Ross, Stroudsburg, PA.

Manning, A.H., J.S. Caine, P.L. Verplanck, D.J. Bove, and K.G. Kahn. 2009. U.S. Geological Survey research in Handcart Gulch, Colorado: An alpine watershed with natural acid-rock drainage quality in central Colorado. In R.M.T. Webb and D.J. Semmens, eds. Planning for an uncertain future: Monitoring, integration, and adaptation. Proceedings of the Third Interagency Conference on

Research in the Watersheds, pp. 97–102. U.S. Geological Survey Scientific Investigations Report 2009-5049.

Manning, A.H., M.J. Friedel, P.L. Verplanck, and A.S. Todd. 2010. Applying numerical modeling to evaluate the significance of climate and hydrology in the formation of natural acid-rock drainage in mineralized watersheds. Geological Society of America Abstracts with Programs 42(5):214.

Markstrom, S.L., L.E. Hay, C.D. Ward-Garrison, J.C. Risley, W.A. Battaglin, D.M. Bjerklie, K.J. Chase, D.E. Christiansen, R.W. Dudley, R.J. Hunt, K.M. Koczot, M.C. Mastin, R.S. Regan, R.J. Viger, K.C. Vining, and J.F. Walker. In press. Integrated watershed-scale response to climate change for selected basins across the United States: U.S. Geological Survey Scientific Investigations Report 2011–5077.

Mast, M.A. 1992. Geochemical Characteristics. In J. Baron, ed. Biogeochemistry of Subalpine Ecosystem: Loch Vale Watershed, pp. 93–107. Springer-Verlag, New York.

National Atmospheric Deposition Program (NRSP-3). 2007. NADP Program Office, Illinois State Water Survey, 2204 Griffith Dr., Champaign, IL 61820. http://nadp.sws.uiuc.edu/

Parkhurst, D.L., and C.A.J. Appelo. 1999. User's guide to PHREEQC (version 2): A computer program for speciation, batch-reaction, one-dimensional transport and inverse geochemical calculations. U. S. Geological Survey Water-Resources Investigations Report 99-4259.

Pederson, G.T., S.T. Gray, C.A. Woodhouse, J.L. Betancourt, D.B. Fagre, J.S. Littell, E. Watson, B.H. Luckman, and L.J. Graumlich. 2011. The unusual nature of recent snowpack declines in the North American cordillera. Science 333(6040):332–335, doi:10.1126/science.1201570. http://www.sciencemag.org/content/333/6040/332. Accessed 6 September 2011.

Schmidt, T.S., S.E. Church, W.H. Clements, K.A. Mitchell, D.L. Fey, R.B. Wanty, P.L. Verplanck, C.A. San Juan, T.L. Klein, E.H. DeWitt, and B.W. Rockwell. 2009. Aquatic ecosystems in central Colorado are influenced by mineral forming processes and historical mining. In R.M.T. Webb and D.J. Semmens, eds. Planning for an uncertain future: Monitoring, integration, and adaptation. Proceedings of the Third Interagency Conference on Research in the Watersheds, pp. 195–205. U.S. Geological Survey Scientific Investigations Report 2009-5049.

Trenberth, K.E., A. Dai, R.M. Rasmussen, and D.B. Parsons. 2003. The changing character of precipitation. Bulletin of the American Meteorological Society 84:1205–1217.

Webb, R.M.T., J.I. Linard, and M.E. Wieczorek. 2006. The water, energy, and biogeochemical model (WEBMOD): A TOPMODEL application developed within the modular modeling system. In Proceedings of the 3rd Federal Interagency Hydrologic Modeling Conference, Reno, NV, 2–6 April 2006, 8 pp. Advisory Committee on Water Information, Subcommittee on Hydrology. [online] URL: http://acwi.gov/hydrology/mtsconfwkshops/conf_proceedings/3rdFIHMC/3D_Webb1.pdf. Accessed 6 Sept 2011.

Williamson, M.A., and J.D. Rimstidt. 1994. The kinetics and electrochemical rate-determining step of aqueous pyrite oxidation. Geochimica et Cosmochimica Acta 58(24):5443–5454.

Wolock, D.M. 1993. Simulating the variable-source-area concept of streamflow generation with the watershed model TOPMODEL. U.S. Geological Survey Water-Resources Investigations Report 93-412.

Utilizing Long-Term ARS Data to Compare and Contrast Hydroclimatic Trends from Snow and Rainfall Dominated Watersheds

D.C. Goodrich, D. Marks, M.S. Seyfried, T.O. Keefer, C.L. Unkrich, E.A. Anson, P.E. Clark, G.N. Flerchinger, E.P. Hamerlynck, S.P. Hardegree, P. Heilman, C. Holifield-Collins, M.S. Moran, M.A. Nearing, M.H. Nichols, F.B. Pierson, R.L. Scott, J.J. Stone, S.S. Van Vactor, A.H. Winstral, J.K. Wong

Abstract

The U.S. Department of Agriculture–Agricultural Research Service, Northwest and Southwest Watershed Research Centers have operated the Reynolds Creek Experimental Watershed (RCEW) in southwestern Idaho and the Walnut Gulch Experimental Watershed (WGEW) in southern Arizona since the 1950s. Each watershed is densely instrumented with a variety of hydrometeorological instrumentation and has multiple gauged subwatersheds spanning a range of spatial scales. These watersheds have yielded an extensive knowledge base of watershed processes over multiple decades of use as outdoor hydrologic laboratories. Both research centers have published data reports in *Water Resources Research* describing the RCEW and WGEW and their associated characteristics and observational databases. Precipitation and runoff generation in RCEW is dominated by snow and snowmelt processes, while WGEW is dominated by thunderstorm-generated rainfall during the summer monsoon. Mean annual temperatures in the continental United States have increased from 1 to 3°C since the establishment of these experimental watersheds and this change has affected water supply, hydrology, and watershed response at both locations. This study compared and contrasted hydroclimatic variables at these experimental watersheds, including temperature, precipitation, and streamflow. Monthly, seasonal, and annual data of temperature, precipitation and runoff were tested for significant trends in these variables.

Keywords: experimental watersheds, trends, temperature, precipitation, runoff

Goodrich, Anson, Hamerlynck, Heilman, Holifield-Collins, Keefer, Moran, Nearing, Nichols, Scott, Stone, Unkrich, and Wong are with the U.S. Department of Agriculture–Agricultural Research Service (USDA–ARS) Southwest Watershed Research Center, 2000 E. Allen Rd., Tucson, AZ 85719. Email: dave.goodrich@ars.usda.gov, eric.anson@ars.usda.gov, erik.hamerlynck@ars.usda.gov, phil.heilman@ars.usda.gov, chandra.holifield@ars.usda.gov, tim.keefer@ars.usda.gov, susan.moran@ars.usda.gov, mark.nearing@ars.usda.gov, mary.nichols@ars.usda.gov, russ.scott@ars.usda.gov, jeff.stone@ars.usda.gov, carl.unkrich@ars.usda.gov, jason.wong@ars.usda.gov. Marks, Clark, Flerchinger, Hardegree, Pierson, Seyfried, Van Vactor, and Winstral are with the USDA-ARS Northwest Watershed Research Center, 800 Park Blvd., Suite 10, Boise, ID 83712. Email: arsdanny@gmail.com, pat.clark@ars.usda.gov, gerald.flerchinger@ars.usda.gov, stuart.hardegree@ars.usda.gov, fred.pierson@ars.usda.gov, mark.seyfried@ars.usda.gov, steve.vanvactor@ars.usda.gov, adam.winstral@ars.usda.gov.

Introduction

To understand how variations in climate, land use, and land cover will affect water supply, ecosystems, and natural resources, we must have access to long-term hydrologic and climatic databases. Data from watersheds that include significant human activities, such as grazing, farming, irrigation, and urbanization, are critical for determining the signature of human-induced changes on hydrologic processes and the water cycle. One of the primary components of effective watershed research is a sustained, long-term monitoring and measurement program. The U.S. Department of Agriculture–Agricultural Research Service (USDA–ARS) Experimental Watershed Network is one such example (Goodrich et al. 1994, Slaughter and Richardson 2000). Two of the ARS Experimental

Watersheds in the Western United States will be featured in this study with the intent of expanding the analysis to other ARS watersheds in the future. They are the Reynolds Creek Experimental Watershed (RCEW), a 239-km^2 drainage in southwestern Idaho near Boise, and the Walnut Gulch Experimental Watershed (WGEW; 149 km^2) in southeastern Arizona near the town of Tombstone. These and the other ARS watersheds are operated as outdoor hydrologic laboratories in which watershed research is supported by long-term monitoring of basic hydroclimatic parameters.

RCEW consists of its drainage area and a third-order perennial stream draining north to the Snake River and ranges in elevation from 1,101 m above mean sea level (amsl) to 2,241 m amsl. About 77 percent of the watershed is under public ownership, with the remainder being privately owned. Primary land use of the watershed is livestock grazing with some irrigated fields along the creek at lower elevations. There is wide diversity in local climate, geology, soils, and vegetation across the Reynolds Creek landscape. Annual precipitation varies from 230 mm at the northern lower elevations to over 1,100 mm in the higher southern regions where 75 percent or more of annual precipitation occurs as snowfall. The ecology and hydroclimatology of RCEW are representative of much of the interior mountain west and Great Basin.

WGEW ranges in elevation from 1,220 to 1,950 m amsl. Its streams are ephemeral with uplands of desert shrubs dominating the lower two thirds of the watershed and desert grasses dominating the upper one third. The climate at WGEW is classified as semiarid with a mean annual temperature at Tombstone of 17.7^{o}C and mean annual precipitation of 312 mm. The precipitation regime is dominated by the North American Monsoon with about 60 percent of the annual total coming during July, August, and September. Summer events are localized short-duration, high-intensity convective thunderstorms, and winter storms are generally slower moving frontal systems. Virtually all runoff is generated by summer thunderstorm precipitation and runoff volumes, and peak flow rates vary greatly with area and on an annual basis.

More detailed descriptions of both RCEW and WGEW have been presented in special sets of papers in *Water Resources Research* (Slaughter et al. 2001, Moran et al. 2008). Research at RCEW continues to be supported by monitoring runoff at 9 weirs, 32 primary and 5 secondary meteorological stations, 26 precipitation stations, 8 snow courses and 5 snow study sites, 27 soil temperature and moisture measurement sites with 5 subsurface hill-slope hydrology sites, and 5 eddy covariance systems. WGEW contains 30 instrumented watersheds for runoff, of which 17 also monitor sediment, 88 precipitation gauges, 3 meteorological stations, 2 eddy covariance stations, and 24 soil moisture monitoring sites (5 with depth profiles). The objective of this study is to carefully examine observations common to both experimental watersheds to quantify the magnitude of climate warming and concurrent changes in precipitation and streamflow over the past 40 to 50 years.

Methods

Observations

Observations of daily maximum and minimum temperature (Tmax, Tmin), precipitation, and runoff were selected from RCEW and WGEW for slightly different time periods depending on installation of instrumentation, but most were initiated in the early to mid 1960s. For RCEW, temperature, precipitation, and runoff were analyzed for the period 1962–2006. Because of significant elevation change in RCEW and its importance to rain-snow precipitation phases, three meteorological stations and runoff weirs were selected, covering an elevation range of over 900 m. In RCEW, precipitation, Tmin, and Tmax observations were co-located. The low-elevation site (RC-Low, site 076, elevation 1,207 m) is located in a relatively broad, flat valley bottom only 108 m above, but nearly 10 km distant from, the RCEW outlet weir. Site vegetation is Wyoming big sagebrush and is typical of low elevations in RCEW. The mid-elevation site (RC-mid, site 127) is located on the eastern side of the basin near the midpoint elevation of the watershed (1,718 m). Site vegetation is dominated by low sagebrush and is typical of mid-elevation vegetation on the eastern side of RCEW. The high-elevation site (RC-high, site 176, elevation 2,093 m) is near the southern rim of the RCEW in an exposed area where a few trees and larger shrubs offer limited shelter from the wind. Site vegetation is a mix of shrubs including mountain big sagebrush, snowberry, and buckbrush. Adjacent to the site are Douglas fir and a few Aspen trees.

For WGEW, the long-term temperature observations are located adjacent to the ARS field headquarters in Tombstone. It is also adjacent to a large surface mining operation, and because of concerns about its affect on the temperature recording station, the Tombstone

station was compared to 10 nearby long-term temperature records in Cochise County obtained from the National Climate Data Center. For the period 1961–2009, no significant differences between the Tombstone and adjacent records were found, but to minimize the impact of data gaps (approximately 10 percent of the data are missing) daily data were averaged for the 10 stations, not including any missing values. For precipitation and runoff, three subwatersheds were selected, spanning a range of spatial scales (Table 1). Precipitation records were analyzed for the period 1957–2010 and runoff for the period 1964–2010.

Table 1. Streamflow measurement stations.

Experimental watershed	Name	Elev. (m)	Drainage area (km^2)
RCEW	Reynolds Mtn. East	2,022	0.39
	Tollgate	1,404	55.0
	Outlet	1,099	238.0
WGEW	WG11	1,427	6.35
	WG6	1,334	81.5
	WG1	1,219	131.0

In RCEW, point measurements of precipitation were used from the same meteorological stations where temperature was recorded. For WGEW, areal average precipitation depths were computed over the three subwatersheds using the dense rain gauge network (approx. 0.570 gauges per 1 km^2) according to the procedure described in Goodrich et al. (2008).

Trend Analysis

Each daily time series was aggregated into months, seasons of a water year, and water years for trend analysis. The three-month seasons, starting from the beginning of the water year, are October, November, and December (OND); January, February, and March (JFM); April, May, and June (AMJ); and July, August, and September (JAS). Trends in air temperature, snow, and streamflow data were computed using two methods: least square (LS) linear regression and Sen's slope (SS) estimator. Although the LS method is in common use, the slope of the regression can be sensitive to autocorrelation and extreme values.

To address this problem, Hirsch et al. (1982, 1991) proposed Sen's slope estimator (Sen 1968), a nonparametric method to detect and estimate the magnitude of temporal trends in hydrologic data. This method computes slopes between all data pairs and estimates the overall representative slope as the median value among all possible slope values.

Following the analysis presented by Nayak et al. (2010), significance of these trends will be evaluated using the nonparametric Mann-Kendall statistic at α = 0.10, 0.05, 0.01, and 0.001 levels (Hirsh and Slack 1984, Yue et al. 2002 a). This statistic has the advantage of testing for consistency in the direction of change for temporally ordered data and is unbiased by the magnitude of change. Two methods will be applied to reduce the influence of autocorrelation on statistical significance of trends in time series data. First, the Mann-Kendall test with prewhitening (MK-PW), as suggested by Zhang et al. (2001), will be applied to eliminate the effects of serial correlation in the Mann-Kendall test. Second, the trend free prewhitening (MK-TFPW) approach (Yue et al. 2002 b) will be applied to minimize the effect of the MK-PW approach on the magnitude of the slope and significance of the trend present in the original data series. This approach also nonparametrically scores the significance of the trend with a sequence of symbols from weak to strong— +, *, **, *** —corresponding to the MK-TFPW test at significance levels of α = 0.10, 0.05, 0.01, 0.001, respectively.

Results

Temperature

In Figure 1, the average annual Tmin and Tmax temperatures are plotted as a function of time for the mid-elevation RCEW station (RC-mid, elevation 1,652 m) and for the average of the 10 Cochise County stations in and surrounding WGEW (WG-CC) with computed trend lines from the Sen's slope estimation method.

There was a significant increasing trend in temperature for the annual average series with a slightly stronger trend in the Tmin series (Table 2). At the seasonal level, significant increasing trends in Tmin were observed for all seasons and stations except the RCEW-Low station and the WG-CC stations during the water year season OND. Significant trends in Tmax were weaker in the case of the WG-CC data: MK-TFPW of * instead of ** or ***. In RCEW, the Tmax trends were significant in the summer (JAS) at all three elevations and in the fall (OND) and winter (JFM) at RC-High. In RCEW, the increasing temperatures had a profound effect on changing the phase of precipitation from snow to rain with the mid- and low-elevation

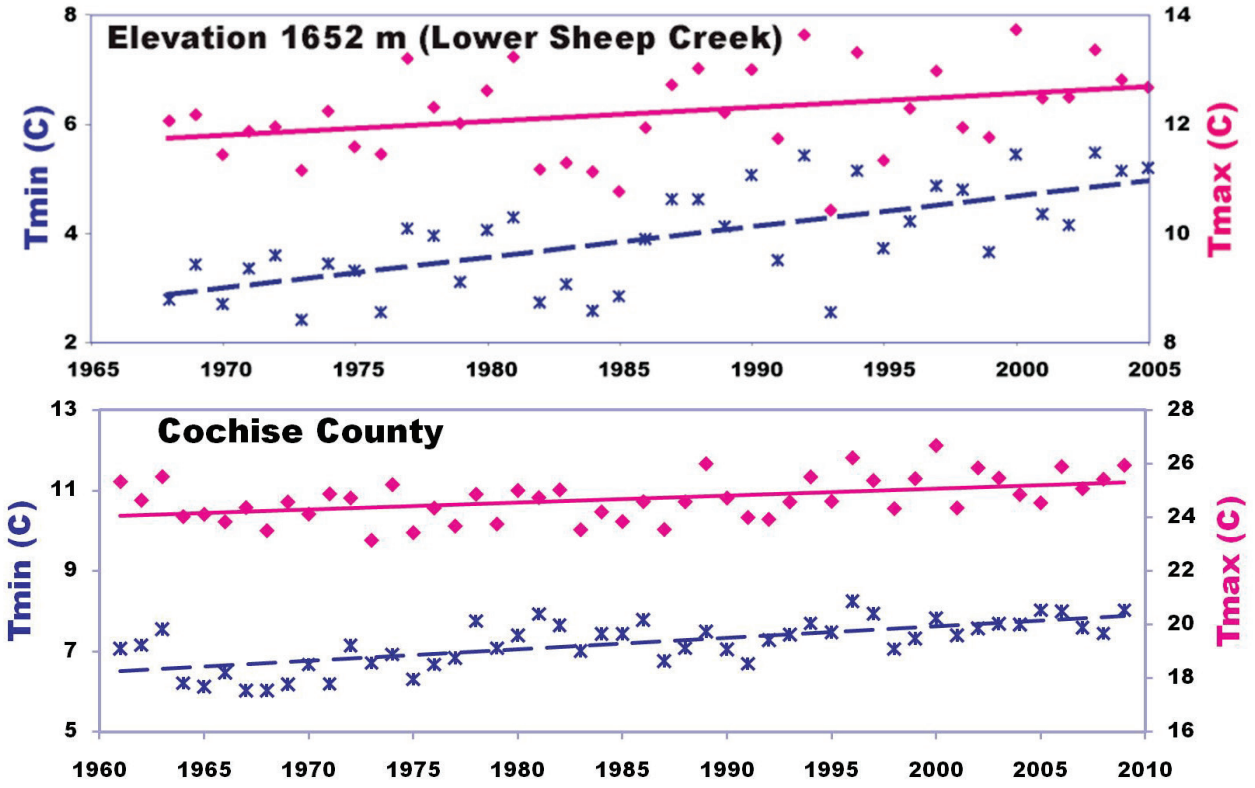

Figure 1. Average annual maximum and minimum daily temperatures for RC-Mid and WG-CC.

stations becoming dominated by rainfall in the later record. Nayak et al. (2010) discusses this result in more detail as well as its effect on snow-water equivalent trends.

Table 2. Annual average trends in Tmin and Tmax.

		Tmin		Tmax	
Station	Elev. (m)	Slope (°C/dec)	Trend sig.[a]	Slope (°C/dec)	Trend sig.[a]
RC-High	2,093	0.45	**	0.35	**
RC-Mid	1,652	0.57	**	0.29	**
RC-Low	1,200	0.36	**	0.20	*
WG-CC[b]	--	0.29	***	0.26	**

[a](MK-TFPW) test significance level: * for α = 0.05, ** for α = 0.01, and *** for α = 0.001

[b]10 Stations in and around the WGEW in Cochise Co.

Precipitation

Very few significant trends in precipitation were detected for either RCEW or WGEW. In WGEW, only a weak (+) to moderately (*) significant trend was found for February precipitation over each of the three subwatersheds. However, precipitation in February comprises just over 5 percent of the annual average and is characterized by low-intensity frontal storms that rarely generate any runoff. An increasing trend in non-summer precipitation for a group of WGEW raingages for the period from 1956 to 1996 was also found by Nichols et al. (2002). However, when an additional 10 years of data were analyzed by Goodrich et al. (2008), there was no trend, due to the influence of multiyear droughts in the more recent data.

Few statistically significant temporal trends (α = 0.10) were found in RCEW. A slight decline during the summer months of approximately 1 percent was the only significant trend. Note that summer precipitation represents a small fraction of annual precipitation, so the affect on other seasons is not significant (at the 90-percent level). The decrease in summer precipitation represents a redistribution of water year precipitation to fall and spring at mid to high elevations (Nayak et al. 2010).

Runoff

At RCEW, most of the flow during a water year occurs from March to June. During these months, nearly 90 percent of annual streamflow occurs at the high-elevation Reynolds Mountain East (RME) weir, 82 percent at the mid-elevation Tollgate (TG) weir, and 70 percent at the RCEW outlet weir. Variation of annual runoff volume is very large, with standard deviations of

at least 50 percent of the annual mean at all sites. The Sen's slope values were negative over the 1962–2006 period of record for all three weirs (Table 3). However there were no significant temporal trends. At the monthly scale, streamflow has shifted toward earlier periods with a shift to late winter and early spring flows at the RME and TG weirs. Streamflow has increased in March and April and decreased in May and June. At the RCEW outlet weir, consistency in trends is less conclusive, with an increase in May flow as the only significant trend (* with $\alpha = 0.05$). It should be noted that spring and summer diversions to irrigation below the TG weir likely confounded trend analysis at the outlet weir. Examined in the context of elevation, there is a strong gradient to this shift. The high-elevation RME weir exhibits a weak but significant (+ with $\alpha = 0.10$) increase in flow in March and April, but the mid-elevation TG weir has significant (* with $\alpha = 0.05$) increase in April flow. The outlet weir exhibits a significant (*) increase in flow in May (Nayak et al. 2010).

Table 3. Water year stream discharge trends.

Watershed	Mean (10^6 m^3/WY)	Stream discharge	Sen's slope (10^6 m^3/decade)
Reynolds Mtn. East	0.21	0.10	–0.008
Tollgate	13.4	7.5	–0.75
Outlet	17.1	12.4	–1.66
WG11	0.066	0.10	–0.013
WG6	0.40	0.44	–0.040
WG1	0.37	0.38	–0.038

In WGEW, on average, there are roughly nine runoff events per year from each of the subwatersheds. Virtually all runoff occurs from the summer monsoon, and infrequent runoff occurs in the early fall as a result of tropical cyclones. While the onset of the monsoon is variable from year to year, the summer months of July, August, and September (JAS) typically contain the monsoon season and therefore almost all runoff production. Like RCEW, the Sen's slope values were negative over the 1964–2010 period of record for all three subwatersheds during this season (Table 3). The trends for WG1 and WG11 were found to be weakly (+) and moderately (**) significant, respectively, and the trend for WG6 was not significant. At the monthly level, a strongly significant (**) decreasing trend was found for all three subwatersheds for the month of September, which appears to be counterintuitive to the findings of Grantz et al. (2007). They found a significant delay in all stages of the monsoon in recent decades with a decrease in rainfall during July and an increase in rainfall during August and September. However, intrastorm precipitation intensity is the primary determinant of runoff generation.

Conclusions

RCEW and WGEW both exhibit moderate to strongly significant trends of increasing temperature that are in agreement with other studies of temperature trends in the western United States and Canada (e.g., Trenberth et al. 2007). The rate of increase in Tmin at the annual temporal scale (+0.29 to 0.57°C per decade) is greater than Tmax (+0.2 to +0.35°C per decade). In RCEW, this has resulted in the crossing of important thermal thresholds. Consequently, the snow season is at least a month shorter than it was in the mid 1960s (Nayak et al. 2010). As rain becomes a larger proportion of the total annual precipitation, runoff occurs earlier in the year.

Changes in precipitation and runoff in the WGEW were less pronounced. While there were moderately significant trends of decreasing runoff in September, it is unclear if this is related to changes in the seasonal onset of the monsoon or a change in rainfall intensity. These decreases will be investigated in more detail in future work. Sensitivity of watershed response will also be examined using runoff to rainfall ratios for each of the watersheds. This study will require improved methods to determine the spatial distribution of precipitation, which is especially challenging in the RCEW where wind-driven redistribution of snow is common. Trends in extremes will also be investigated. Extension of this work to ARS and other experimental watersheds across a wide range of hydroclimatic regions will then be undertaken.

References

Goodrich, D.C., P.J. Starks, R.R. Schnabel, and D.D. Bosch. 1994. Effective use of USDA–ARS experimental watersheds. In Proceedings of the ARS Conference on Hydrology, Denver, CO, 13–15 September 1993, pp. 35–46. U.S. Department of Agriculture, Agricultural Research Service, Publication 1994-5.

Goodrich, D.C., C.L. Unkrich, T.O. Keefer, M.H. Nichols, J.J. Stone, L. Levick, and R.L. Scott. 2008.

Event to multidecadal persistence in rainfall and runoff in southeast Arizona. Water Resources Research 44:W05S14, doi:10.1029/2007WR006222.

Grantz, K., B. Rajagopalan, M. Clark, and E. Zagona. 2007. Seasonal shifts in the North American monsoon. Journal of Climate 20:1923–1935, doi:10.1175/JCLI4091.1.

Hirsch, R.M., R.B. Alexander, and R.A. Smith. 1991. Selection of methods for the detection and estimation of trends in water quality. Water Resources Research 27(5):803–813, doi:10.1029/91WR00259.

Hirsch, R.M., and J.R. Slack. 1984. A nonparametric trend test for seasonal data with serial dependence. Water Resources Research 20(6):727–732, doi:10.1029/WR020i006p00727.

Hirsch, R.M., J.R. Slack, and R.A. Smith. 1982. Techniques of trend analysis for monthly water quality data. Water Resources Research 18(1):107–121, doi:10.1029/WR018i001p00107.

Moran, M.S., W.E. Emmerich, D.C. Goodrich, P. Heilman, C. Holifield Collins, T.O. Keefer, M.A. Nearing, M.H. Nichols, K.G. Renard, R.L. Scott, J.R. Smith, J.J. Stone, C.L. Unkrich, and J.K. Wong. 2008. Preface to special section on fifty years of research and data collection: U.S. Department of Agriculture Walnut Gulch Experimental Watershed. Water Resources Research 44:W05S01, doi:10.1029/2007WR006083.

Nayak, A., D. Marks, D. Chandler, and M. Seyfried. 2010. Long-term snow, climate and streamflow trends from at the Reynolds Creek Experimental Watershed, Owyhee Mountains, Idaho, USA. Water Resources Research 46:W06519, doi: 10.1029/2008WR007525.

Nichols, M.H., K.G. Renard, and H.B. Osborn. 2002. Precipitation changes from 1956–1996 on the Walnut Gulch Experimental Watershed. Journal of the American Water Resources Association 38(1):161–172.

Sen, P.K. 1968. Estimates of the regression coefficient based on Kendall's tau. Journal of the American Statistical Association 63:1379–1389, doi:10.2307/2285891.

Slaughter, C.W., D. Marks, G.N. Flerchinger, S.S. Van Vactor, and M. Burgess. 2001. Thirty-five years of research data collection at the Reynolds Creek Experimental Watershed, Idaho, United States. Water Resources Research 37(11):2819–2823.

Slaughter, C.W., and C.W. Richardson. 2000. Long term watershed research. Water Resources Impact [U.S. Department of Agriculture, Agricultural Research Service] 2(4):28–31.

Trenberth, K.E., and P.D. Jones. 2007. Observations: Surface and Atmospheric Climate Change. In S. Solomon, D. Qin, M. Manning, Z. Chen, M. Marquis, K.B. Averyt, M. Tignor, and H.L. Miller, eds. Climate Change 2007: The Physical Science Basis. Contribution of Working Group I to the Fourth Assessment Report of the Intergovernmental Panel on Climate Change, pp. 235–336. Cambridge University Press, Cambridge, U.K.

Yue, S., P. Pilon, and G. Cavandias. 2002a. Power of the Mann–Kendall and Spearman's rho tests for detecting monotonic trends in hydrological series. Journal of Hydrology 259(1–4):254–271, doi:10.1016/S0022-1694(01)00594-7.

Yue, S., P. Pilon, B. Phinney, and G. Cavadias. 2002b. The influence of autocorrelation on the ability to detect trend in hydrological series. Hydrologic Processes 16: 1807–1829, doi:10.1002/hyp.1095.

Zhang, X., K.D. Harvey, W.D. Hogg, and T.R. Yuzyk. 2001. Trends in Canadian streamflow. Water Resources Research 37(4):987– 998, doi:10.1029/2000WR900357.

Analysis of Trends in Climate, Streamflow, and Stream Temperature in North Coastal California

M.A. Madej

Abstract

As part of a broader project analyzing trends in climate, streamflow, vegetation, salmon, and ocean conditions in northern California national park units, we compiled average monthly air temperature and precipitation data from 73 climate stations, streamflow data from 21 river gaging stations, and limited stream temperature data from salmon-bearing rivers in north coastal California. Many climate stations show a statistically significant increase in both average maximum and average minimum air temperature in early fall and midwinter during the last century. Concurrently, average September precipitation has decreased. In many coastal rivers, summer low flow has decreased and summer stream temperatures have increased, which affects summer rearing habitat for salmonids. Nevertheless, because vegetative cover has also changed during this time period, we cannot ascribe streamflow changes to climate change without first assessing water budgets. Although shifts in the timing of the centroid of runoff have been documented in snowmelt-dominated watersheds in the western United States, this was not the case in lower elevation coastal rivers analyzed in this study.

Keywords: streamflow, climate, temperature, precipitation, northern California

Introduction

In north coastal California, daily, seasonal, and decadal variations in abiotic drivers (e.g., precipitation, fog, streamflow, and temperatures of air, ocean, and streams) regulate many ecological processes, including the distribution of vegetation and wildlife and frequency of disturbances from fires, floods, landslides, and biotic pests. However, the exact nature of the linkages between abiotic drivers and the direct and indirect effect of these drivers on species of concern and their habitat are not well understood.

In addition to needing greater understanding of the basic linkages between abiotic and biotic ecosystem elements, the question of climate change is of increasing concern to land managers. They need to understand how climate change has already affected natural resources and whether other changes may be looming. Without this understanding it is increasingly difficult to judge the effects of management efforts (e.g., stream restoration), evaluate the resilience of existing habitats, or plan future management actions.

Complicating a manager's ability to respond to climate change effects is the common assumption of stationarity—the idea that natural systems fluctuate within an unchanging envelope of variability (Milly et al. 2008). The stationarity assumption is being compromised by major shifts in background environmental conditions. These major shifts may be changing the timing, magnitude, and intensity of critical abiotic elements in this region. In addition, the common assumption that restoration planning can use historical reference conditions as a goal may not be valid if extrinsic drivers display nonstationarity. Consequently, the understanding of trends, variability, and interactions among abiotic drivers is needed to inform restoration strategies, prioritize restoration sites, and implement scenario planning to foster strategic thinking about future conditions and management alternatives.

The National Park Service (NPS), through its Inventory and Monitoring Program, has monitored many abiotic drivers and has conducted several biological surveys. A major concern is the decline of salmon populations in coastal California park streams. In central and northern California, several salmon and steelhead populations have been in decline for years and many are federally listed as threatened or endangered. In 1997, coho salmon *(Oncorhynchus kisutch)* were federally listed as

Madej is a research geologist with the U.S. Geological Survey, Arcata, CA 95521. Email: mary_ann_madej@usgs.gov.

Table 1. Gaging stations used in analysis.

Station name	Agency	County	Period of record (water years)	Drainage area (km^2)
Bull Creek near Weott	USGS	Humboldt	1961–2010	72.8
Eel River at Scotia[1]	USGS	Humboldt	1911–2010	8,062.7
Elder Creek near Branscomb	USGS	Mendocino	1968–2009	16.8
Lacks Creek	USGS/NPS	Humboldt	1981–2010	43.8
Little Lost Man Creek near Orick	USGS/NPS	Humboldt	1975–2010	9.0
Little River near Trinidad	USGS	Humboldt	1956–2010	104.9
Mad River near Arcata[2]	USGS	Humboldt	1951–2010	1,256.2
Mattole River near Petrolia	USGS	Humboldt	1951–2010	634.6
North Fork Caspar Creek	USFS[3]	Humboldt	1964–2003	4.7
Olema Creek	NPS	Marin	1998–2010	40.0
Panther Creek near Orick	USGS/NPS	Humboldt	1980–2010	15.7
Prairie Creek above Brown Creek	NPS	Humboldt	1990–2008	10.6
Prairie Creek above May Creek	NPS	Humboldt	1991–2008	32.6
Redwood Creek at O'Kane	USGS	Humboldt	1973–2010	175.3
Redwood Creek at Orick	USGS	Humboldt	1954–2010	720.0
Redwood Creek at GOGA	NPS	Marin	1998–2010	18.1
San Geronimo Creek	MMWD[4]	Marin	1980–2009	24.3
Smith River at Crescent City	USGS	Del Norte	1932–2010	1,590.3
South Fork Caspar Creek	USFS	Humboldt	1964–2003	4.2
South Fork Eel River at Leggett	USGS	Mendocino	1966-2009	642.3
Van Duzen River at Bridgeville	USGS	Humboldt	1951–2008	575.0

[1]Flow regulated by Lake Pillsbury and diversion through Potter Valley power plant at drainage area of 883 km^2
[2]Flow regulated by Ruth Reservoir at drainage area of 313 km^2
[3]U.S. Forest Service Pacific Southwest Research Station
[4]Marin Municipal Water District

threatened in the Southern Oregon/Northern California Evolutionary Significant Unit, including Redwood National Park, and as endangered in the Central California Coast.

Factors affecting coho populations include elevated stream temperatures (Welsh et al. 2001), water withdrawals, dams, loss of spawning and rearing habitat, and extreme hydrologic events (Carlisle et al. 2009). Millions of dollars are being spent in coastal parks on watershed and stream restoration projects. As the NPS plans salmon restoration activities in coastal watersheds, it is critical to understand the abiotic factors and interactions that affect salmonid populations (MacCall and Wainwright 2003, Battin et al. 2007).

The objectives of this study are to identify trends in climate drivers and hydrologic regimes that may be having local and regional effects on salmon populations in north coastal California streams, with an emphasis on four national park units, Redwood National Park (REDW), Golden Gate National Recreation Area (GOGA), Point Reyes National Seashore (PORE), and Muir Woods National Monument (MUWO).

Study Area

The climate and streamflow monitoring stations used in this study are located along the north coast of California from the San Francisco Bay area (37°N) to the Oregon border (42°N). The region has a Mediterranean climate with mild, rainy winters and generally cool, dry summers. Coastal fog is a common occurrence in the summer months. Mean daily minimum temperatures in January range from 0.4 to 7°C and mean daily maxima in July range from 14 to 30°C. Mean annual precipitation is moderate to high, generally more than 100 cm, but as low as 70 cm in the southern part of the region and more than 200 cm in the northern mountains. The region is dominated by the Coast Range, which separates the coastal area from the hotter Central Valley farther inland.

Table 2. P-values for trends in air temperature and precipitation at four national park units.

	REDW[1]	GOGA	PORE	MUWO
Average annual precipitation	0.512	0.906	0.772	0.451
Average annual temperature				
Maximum	0.269	**<0.001**[2]	**<0.001**	**<0.001**
Mean	0.810	**<0.001**	**<0.001**	**<0.001**
Minimum	0.414	**<0.001**	**<0.001**	**<0.001**
Average monthly temperature (maximum)				
January	**0.095**	**<0.001**	**0.002**	**<0.001**
February	0.700	**0.007**	**0.019**	**0.002**
March	0.692	**0.010**	**0.034**	**0.004**
April	**0.027**	0.152	0.123	**0.079**
May	0.960	**0.002**	**0.002**	**0.002**
June	0.257	0.923	0.626	0.993
July	0.854	0.538	0.406	0.287
August	0.214	**<0.001**	**<0.001**	**0.080**
September	0.578	**0.005**	**0.006**	**0.032**
October	0.243	**0.001**	**0.003**	**0.003**
November	**0.022**	0.443	0.762	0.414
December	0.843	**0.042**	0.187	**0.016**

[1]REDW, Redwood National Park; GOGA, Golden Gate National Recreation Area; PORE, Point Reyes National Seashore; MUWO, Muir Woods National Monument

[2]Values in bold show statistically significant increasing trends at the 90% level.

Methods

The PRISM (Parameter-elevation Regressions on Independent Slopes Model) Climate group at Oregon State University provided air temperature and precipitation data. The PRISM group incorporated climate data from specific points (climate stations) and extrapolated those data to describe air temperature and rainfall in selected national park units (http://prismmap.nacse.org/klamath). Long-term trends in maximum, mean, and minimum temperatures and precipitation were examined through linear regression. Streamflow records were obtained for gaging stations operated by the U.S. Geological Survey (USGS), REDW, GOGA, and PORE. Most datasets consisted of mean daily streamflow and peak flows. Streamflow records from 67 gaging stations located along north coastal California were examined. Many of the rivers have altered hydrologic regimes because of impoundments or diversions, and others had short (<10 years) periods of record or large data gaps. Nineteen stations with adequate records and unimpaired flow regimes were retained for more in-depth analysis, as well as two rivers with dams in their headwaters (Table 1). Drainage areas ranged from 4.2 to 8,063 km^2. Some stations also included stream temperature records from in situ temperature data loggers with sampling intervals that ranged from 15 to 60 minutes. Daily maximum, mean, and minimum water temperatures were calculated from these datasets. Following the approach of Gu et al. (1999), we used air temperature and streamflow as independent variables with stream temperature as the dependent variable in a multiple regression analysis. Because salmon migration, spawning, and rearing success are dependent on magnitude and timing of flow, we analyzed the 7-day low flow and the dates of percentiles of cumulative runoff volumes. Cumulative runoff curves were constructed by accumulating mean daily discharge for each water year (WY; October 1–September 30). Various percentiles of runoff could then be calculated. For example, the timing of the center of mass of flow (the date by which 50 percent of the runoff has occurred, or CT) was calculated for each station.

Results

The PRISM results cover the period of 1895 to 2007. Figure 1 shows an example of PRISM output for GOGA. Park units in the San Francisco Bay area (GOGA, MUWO, and PORE) showed a statistically significant increase in annual maximum, mean, and

minimum air temperatures of about 1°C during the last 100 years (Table 2). On a monthly basis, significant increases were detected in January, February, March, May, August, September, and October. Farther north, in REDW, air temperature did not increase significantly. No trend in annual precipitation was detected, but all park units showed statistically significant decrease (at the 90-percent level) in September rainfall during the last century, a decrease of 10 mm in the south and 30 mm in the north.

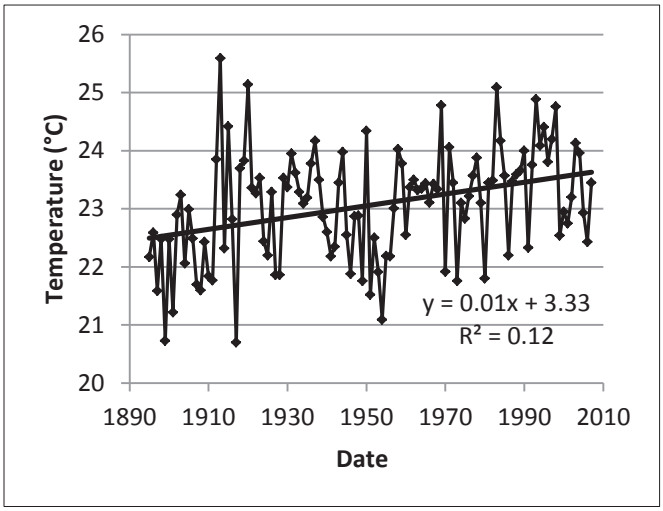

Figure 1. Average daily maximum air temperature for August calculated for GOGA by PRISM.

Timing of runoff was assessed at 21 gaging stations. CT ranged from December to April but commonly occurred in early February (Figure 2). CT was fairly synchronous among watersheds from the San Francisco Bay area north to the Oregon border (Figure 2). Since the late 1940s, CT has shifted towards earlier in the water year in many mountainous rivers of western North America (Stewart et al. 2004). In contrast to trends documented in those mountainous watersheds with large snowmelt components, none of the lower elevation coastal streams in this study showed a significant trend at the 0.10 level of earlier or later runoff based on CT values.

Another streamflow characteristic of concern for fish is summer low flow. The 7-day low flow decreased at 10 of the stations over the period of record. Redwood Creek at Orick is an example of this decrease (Figure 3). Other stations that exhibited a statistically significant decrease at the 90-percent level were Mattole, Van Duzen, and South Fork Eel rivers and Lacks, Olema, North Fork Caspar, Elder, Redwood at O'Kane, and San Geronimo creeks. Statistical significance does not automatically imply a biological significance. Nevertheless, lower flows are associated with less pool volume for summer rearing of salmon or dry river reaches. In addition, solar radiation can heat a smaller mass of water faster than greater water volumes, leading to elevated stream temperatures.

Coho salmon are very sensitive to elevated stream temperatures, and stream temperature tends to peak in late July or early August. The maximum weekly average temperature (MWAT) in the southern streams (Olema Creek in PORE and Redwood Creek in GOGA) ranged from 14.2°C in WY2010 to 19.1°C in WY2006, based on measurements from WY2003 to 2010. MWATs in Prairie Creek above May Creek in REDW were somewhat cooler, ranging from 13.1°C to 15.8°C from WY1997 to 2010. In contrast, MWATs in Redwood Creek at O'Kane were consistently above 16.8°C, the temperature restriction for coho assessed by Welsh et al. (2001). At this station MWATs ranged from 19.8°C to 23.9°C, based on measurements from WY1997 to 2010.

The relationship between air temperature (as a surrogate for solar radiation, which directly affects water temperature) and stream temperature was assessed for Redwood Creek near the O'Kane gaging station, where several years of air and stream temperature data were available (Sparkman, California Department of Fish and Game, personal commun.). For the months of June, July, and August, daily maximum stream temperature was strongly correlated with both daily maximum air temperature and mean daily streamflow at the gaging station ($n = 400$, $r^2 = 81$ percent, p-value <0.0001).

Discussion

Gaging station records have different periods of record, so a full statistical comparison among the stations could not be done. Consequently, the trends noted in this paper should be considered a starting point for more in-depth analyses in specific watersheds. For example, a decrease in summer low flows can be problematic for salmonid habitat, but it cannot simply be ascribed to climate change without assessing other possible influences. Minor diversions for domestic or agricultural use are not quantified, and some illegal water diversions may also influence summer low flows. Sedimentation in river beds may cause surface runoff to go subsurface, decreasing the amount of available surface flow in the summer. Regrowth of trees in formerly logged watersheds can increase the evapotranspiration demand and decrease summer low flow (Reid and Lewis, in press). A decrease in summer

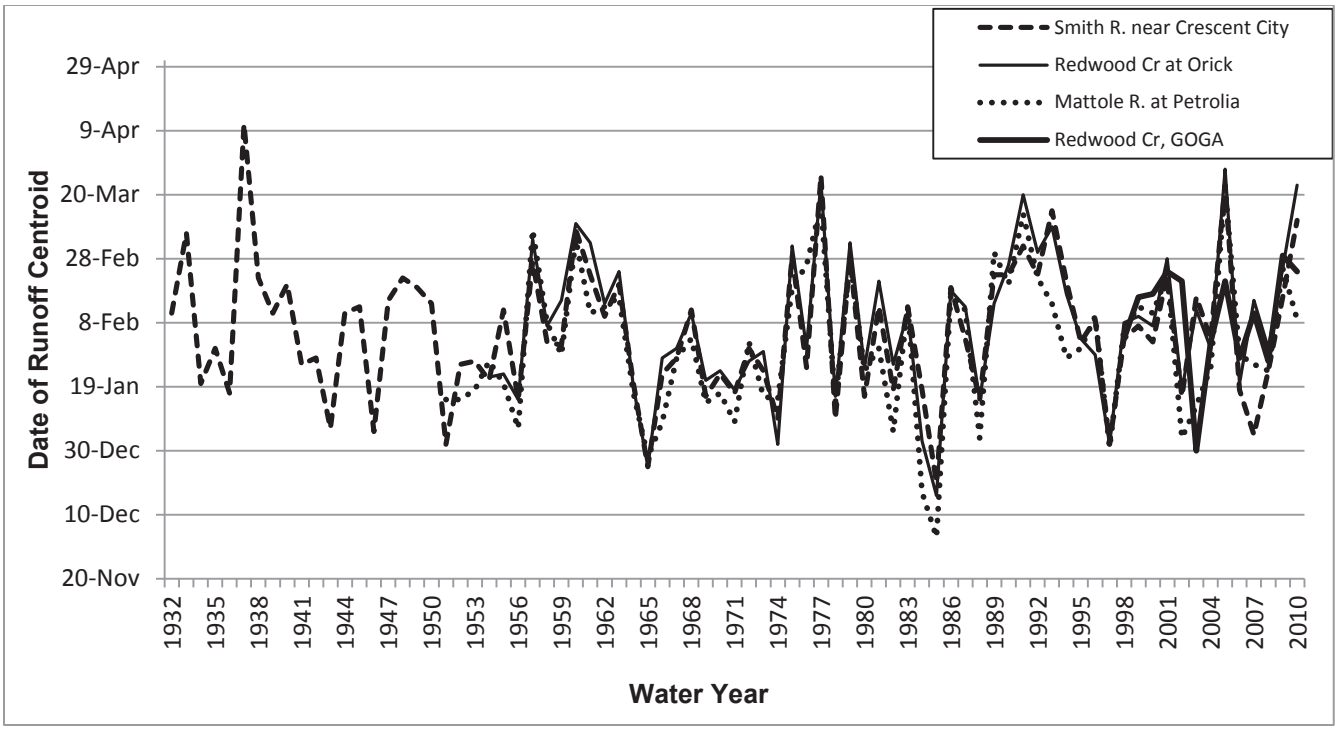

Figure 2. Timing of runoff centroid for four rivers, spanning the coastal region from the Oregon border (Smith River near Crescent City) to the San Francisco Bay area (Redwood Creek at GOGA).

fog can also increase the evapotranspiration demand. Preliminary analysis of fog frequency at two sites within the study area suggests a decrease in fog in recent years (Johnstone and Dawson 2010). Nevertheless, the full spatial and temporal distribution of fog is not known, and further analysis based on remote sensing data of coastal fog is in progress. Future research will also assess changes in vegetative cover during the period of streamflow records.

Interannual variations in climate are linked to the El Niño/Southern Oscillation phenomenon (ENSO). Annual flood peaks in coastal rivers at the north end of our study area are significantly smaller during El Niño conditions; south of 35°N (south of San Francisco) they are significantly larger during an El Niño phase (Andrews and others 2004). Future research will examine trends in other aspects of runoff (in CT, low flows, etc.) with respect to ENSO events.
Elevated stream temperatures in Redwood Creek at O'Kane in 2006 and 2009 led to fish kills (Sparkman, California Department of Fish and Game, personal commun.), and stream temperatures at many locations along Redwood Creek in REDW are above the temperatures preferred by coho (Welsh et al. 2001, Madej et al. 2006). Increases in stream temperature can be exacerbated by the diversion of streamflow for agriculture or other uses, or if reduced rainfall decreases summer baseflow. Consequently, if air temperature increases or summer flow decreases, we can expect warmer summer stream temperatures, adding to stressful conditions for summer-rearing salmonids and for unique runs of adult summer steelhead holding in pools throughout the summer.

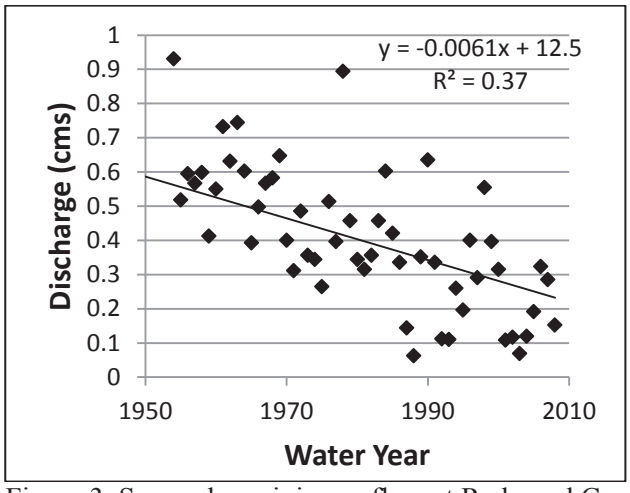

Figure 3. Seven-day minimum flow at Redwood Creek at Orick, USGS Station #11482500.

Conclusions

The PRISM climate data for four national park units in north coastal California show increases in annual maximum, mean, and minimum air temperatures of

about 1°C during the last century for the three sites near San Francisco Bay, but not at Redwood National Park farther north. September rainfall has decreased at all four units over this same time period. Summer low flow has decreased in several streams in this region, although the causes for the decrease are not fully understood. Daily maximum stream temperature is correlated with daily maximum air temperature and mean daily streamflow. Maximum weekly average stream temperatures in some of the streams exceeded the value preferred by coho salmon (<16.8°C).

Acknowledgments

Numerous staff from the National Park Service provided monitoring data incorporated into this study. Alicia Torregrosa and Andrea Woodward of the USGS helped design the broader project linking abiotic factors to salmon populations. Monica Bueno and Rachel Baker-de Kater compiled and organized reams of data. This project was partially funded by National Park Service–U.S. Geological Survey Vital Signs Synthesis Program. Randy Klein and Vicki Ozaki offered several useful suggestions on an earlier draft of the paper. The use of trade names is for descriptive purposes only and does not imply endorsement by the U.S. Government.

References

Andrews, E.D., R.C. Antweiler, P.J. Neiman, and F.M. Ralph. 2004. Influence of ENSO on flood frequency along the California coast. Journal of Climate 17:337–348.

Battin, J., M.W. Wiley, M.H. Ruckelshaus, R.N. Palmer, E. Korb, K.K. Bartz, and H. Imaki. 2007. Projected impacts of climate change on salmon habitat restoration. Proceedings of the National Academy of Sciences 104(16):6720–6725.

Carlisle, S., M. Reichmuth, E. Brown, and C. del Real. 2009. Long-term coho salmon and steelhead trout monitoring in coastal Marin County 2007: Annual monitoring progress report. National Park Service, Natural Resource Technical Report NPS/SFAN/NRTR-2009/269.

Gu, R., R. McCutcheon, and D.J. Chen. 1999. Development of weather-dependent flow requirements for river temperature control. Environmental Management 24:529–540.

Johnstone, J.A., and T.E. Dawson. 2010. Climatic context and ecological implications of summer fog decline in the coast redwood region. Proceedings of the National Academy of Sciences 107(10):4533–4538, doi:10.1073/pnas.0915062107.

MacCall, A.D., and T.C. Wainwright, eds. 2003. Assessing extinction risk for west coast salmon: Proceedings of the workshop, Seattle, WA, 13–15 November 1996. NOAA Technical Memorandum NMFS-NWFSC-56.

Madej, M.A., C. Currens, V. Ozaki, J. Yee, and D. Anderson. 2006. Assessing possible thermal rearing restrictions for juvenile coho salmon in Redwood Creek, California, through thermal infra-red (TIR) imaging and in-stream monitoring. Canadian Journal of Fisheries and Aquatic Sciences 63:1384–1396.

Milly, P.C.D., J. Betancourt, M. Falkenmark, R.M. Hirsch, Z.W. Kundzewicz, D.P. Lettenmaier, and R.J. Stouffer. 2008. Stationarity is dead: Whither water management? Science 319:573–574.

Reid, L.M., and J. Lewis. In press. Evaluating cumulative effects of logging and potential climate change on dry-season flow in a coast redwood forest**.** In Proceedings of the 4th Interagency Conference on Research in Watersheds, Fairbanks, AK, 26–30 September 2011. [This volume].

Stewart, I.R., D.R. Cayan, and M.D. Dettinger. 2004. Changes in snowmelt runoff timing in Western North America under a 'Business as usual' climate change scenario. Climatic Change 62:217–232.

Welsh, Jr., H.H., G.R. Hodgson, B.C. Harvey, and M.E. Rocher. 2001. Distribution of juvenile coho salmon in relation to water temperatures in tributaries of the Mattole River, California. North American Journal of Fish Management 21:464–470.

Evidence of Climate Change in the Streamflow and Water Temperature Record in the Missouri River Basin

M.T. Anderson, J.F. Stamm, P.A. Norton, J.B. Warner

Abstract

The streamflow and water temperature record was examined for evidence of changing climate conditions in the Missouri River Basin (MRB). Observations of 52 years of continuous record (1957–2008) at about 200 U.S. Geological Survey (USGS) gages indicate that streamflow conditions are changing in the MRB. Trends are evident in the annual mean discharge using the non-parametric Kendall Tau test. There is a strong geographic distribution of the trends, which are generally upward in the eastern and downward in the western parts of the basin. For example, most significant trends ($p \geq 0.10$) are upward at stations in Colorado, North Dakota, South Dakota, Iowa, and Missouri, whereas most significant trends ($p \geq 0.10$) are downward at stations in the mountain west (Montana and Wyoming). The reduced runoff in the western basin has resulted in depleted storage in mainstem reservoirs on the Missouri River for most of the last decade. In addition to mean annual streamflow, mean monthly trends have also changed for many stations. A simple shift of flow, however, from one season to another is not apparent, but trends, both upward and downward, occur across many or all months of the year. The amount of water that these trends of recent decades represent, compared to earlier decades, is profound in some cases. The historical record of water temperature for the Missouri River was compiled and examined for evidence of changing conditions. The long-term records examined consisted of three USGS stations—Missouri River at Toston, Mont. (station 06054500), Missouri River below Garrison Dam, N. Dak. (stations 06339000 and 06338490), and Missouri River at Nebraska City, Nebr. (station 06807000)—and reservoir outflow records collected by the U.S. Corps of Engineers at Garrison Dam in North Dakota and Oahe and Gavins Point Dams in South Dakota. All available data were examined for evidence of water temperature change for two indicator parameters: (1) long-term change over the respective period of record, and (2) any change in the date of the annual maximum temperature. Some evidence exists that the river is warming over time, especially for the reach downstream from the reservoirs, as indicated by the Missouri River station at Nebraska City.

Anderson, Stamm, Norton, and Warner are scientists with the U.S. Geological Survey, South Dakota Water Science Center, 1608 Mountain View Road, Rapid City, SD 57702. Email: manders@usgs.gov, jstamm@usgs.gov, pnorton@usgs.gov, jwarner@usgs.gov.

Long-Term Climate Change Controls Stream and Riparian Area Response to Disturbance in the Semiarid Great Basin

J.C. Chambers

Abstract

Climate change can have long-term effects on watershed geomorphology and, thus, on stream channel processes and riparian ecosystem dynamics. In the central Great Basin, paleoecological and geomorphic reconstructions show that drought conditions coupled with wildfires from 2,500 to 1,900 YBP (years before present) resulted in hillslope erosion and sediment deposition in valley bottoms and on side-valley alluvial fans. Because the hillslopes were depleted of sediment, the subsequent trend has been towards channel incision during flood events. The rate and magnitude of incision has been accelerated by anthropogenic disturbances like roads in the valley bottoms. At watershed scales, basin lithology and geomorphometry determine the long-term response of the basins to disturbance and, thus, the extent and composition of riparian vegetation. Watersheds dominated by volcanic rocks are rugged, have high stream power and hypsometric integrals, and are dominated by disturbance-tolerant woody riparian vegetation. Those dominated by sedimentary and metasedimentary rocks have low stream power and hypsometric integrals, are strongly influenced by side-valley alluvial fans, and have stepped-valley profiles that support a high proportion of meadow ecosystems. At local or stream reach scales, the hydrogeomorphic setting determines the response of streams and riparian ecosystems to disturbance and is reflected in the degree of incision and the structure and composition of the riparian vegetation and aquatic biota. Many of the watersheds have adjusted to the new sediment regime, but many others are functioning as non-equilibrium systems. Development of effective management strategies for these watersheds requires an understanding of the long-term effects of climate and the processes controlling the current responses of the streams and riparian ecosystems to disturbance.

Chambers is a research scientist with the U.S. Department of Agriculture, Forest Service, 920 Valley Road, Reno, NV 89509. Email: jchambers@fs.fed.us.